High Pressure Research

ISSN: 0895-7959 (Print) 1477-2299 (Online) Journal homepage: http://www.tandfonline.com/loi/ghpr20

Evaluation of high hydrostatic pressure effects on bovine red blood cells and platelets

Cagatay Ceylan , Mete Severcan , Faruk Bozoglu & Feride Severcan

To cite this article: Cagatay Ceylan , Mete Severcan , Faruk Bozoglu & Feride Severcan (2009) Evaluation of high hydrostatic pressure effects on bovine red blood cells and platelets, High Pressure Research, 29:2, 358-368, DOI: 10.1080/08957950902941014

To link to this article: http://dx.doi.org/10.1080/08957950902941014

High Pressure Research
Vol. 29, No. 2, June 2009, 358–368

Taylor & Francis
Taylor & Francis Group

Evaluation of high hydrostatic pressure effects on bovine red blood cells and platelets

Cagatay Ceylan[a†], Mete Severcan[b], Faruk Bozoglu[c] and Feride Severcan[d]*

[a]*Department of Biotechnology, Middle East Technical University, Ankara, Turkey;* [b]*Department of Electrical Engineering, Middle East Technical University, Ankara, Turkey;* [c]*Department of Food Engineering, Middle East Technical University, Ankara, Turkey;* [d]*Department of Biological Sciences, Middle East Technical University, Ankara, Turkey*

(*Received 4 October 2008; final version received 2 April 2009*)

The objective of this study was to investigate the effects of high hydrostatic pressure (HHP) on the stability of red blood cells (RBCs) and platelets. Bovine blood cells ($n = 5$) were treated with the pressure of 55, 110, 154 and 220 MPa at 25 °C for 5 min. Light microscopy, atomic force microscopy and flow cytometry studies revealed that RBCs were morphologically stable up until the 220 MPa pressure treatments, at which surface modifications were observed. The platelets were found to be less stable than RBCs. HHP application did not cause any significant change in the signal intensity, band area and frequency values of the infrared bands with the exception that a significant variation was observed in the area of the cholesterol band. No statistically significant variations were observed in the secondary structure elements due to HHP treatment according to the artificial neural network study based on the FTIR data.

Keywords: high hydrostatic pressure (HHP); blood; Fourier transform infrared spectroscopy (FTIR); flow cytometry (FC); atomic force microscopy (AFM)

1. Introduction

High hydrostatic pressure (HHP) treatment has been used advantageously in many areas due to its isostatic pressure properties [1]. One such area where industrial applications already exist is food processing [2]. HHP has been proposed as an alternative technique to thermal processing in order to destroy food-borne pathogens, since it can inactivate or injure microorganisms without altering the flavor and nutrient content of foods [3]. HHP has also been used to develop cancer vaccines to combat this deadly disease [4]. Application of high pressure to membranes is another interesting research area [5]. Moreover, HHP application turns out to be one of the most promising tools that scientists have been using to understand the protein–protein interactions and protein folding and dynamics because high-pressure experiments provide the opportunity to separate the effects of density and temperature on proteins [6].

*Corresponding author. Email: feride@metu.edu.tr
†Present address: Department of Food Engineering, Izmir Institute of Technology, Izmir, Turkey.

ISSN 0895-7959 print/ISSN 1477-2299 online

DOI: 10.1080/08957950902941014
http://www.informaworld.com

The use of HHP makes it also possible to control the dissociation of icosahedral virus capsids, oligomeric proteins, and other sub-cellular assemblies [7]. The inactivation of viruses using HHP treatment has been investigated in various studies [7–9], including one carried out in blood plasma [10].

As a food ingredient, porcine blood fractions treated with HHP reduced the level of contaminant microorganisms while retaining some of the functional properties, such as color properties, protein solubility, foaming and emulsifying properties, texture and water holding capacity [11–13]. Unfortunately, HHP treatments resulted in a considerable increase in hemolysis of RBC and a decrease in platelet numbers and gel formation [14]. The aim of the current study was to analyze the structural effects of HHP treatment on bovine RBCs and platelets, which was achieved using light microscopy for general inspection, atomic force microscopy (AFM) for the detailed analysis of the surface morphology and Fourier transform infrared spectroscopy (FTIR) for monitoring molecular changes. FTIR is a rapid, sensitive, inexpensive and non-destructive method, which is widely used in the analysis of biological systems in any physical state [15,16]. The method allows the analyses of the minute amounts of samples in a short time, with many different digital manipulations of the data.

2. Materials and methods

2.1. *HHP treatments of samples*

The HHP experiments were carried out in a designed and constructed lab-scale unit (capacity 30 cm^3) high pressure cell, where a mixture of deionized water and glycol was used as the isostatic pressure transducing medium. The equipment consists of a pressure chamber of cylindrical design, two end closures, a means for restraining the end closures, a pressure pump and a hydraulic unit to generate high pressure for system compression and also a temperature-control device. The pressure vessel was made of hot galvanized carbon steel and the piston was hard chrome plated and polished to mirror finish (steel type heat treated special K) which was processed into the required sizes at the Electrical and Electronic Engineering Department of Middle East Technical University, Ankara, Turkey. Prior to pressurization, the liquid was heated to the desired temperature by an electrical heating system surrounding the chamber. The rate of pressure increase and pressure release was approximately 5–10 s for the designed system. Throughout the experiments, the samples were subjected to HHP treatment for 5 min at 25 °C. Pressurization times reported in this study did not include the pressure increase and release times. The unit is capable of operating up to 450 MPa pressure between 25–95 °C. The samples were dispensed in 2 ml portions in sterile plastic cryovials without any head space (Sterilin, UK) in duplicate. The operation conditions reported in the previous HHP studies were followed [17].

2.2. *Blood material*

The blood used in this research was post-mortem bovine blood. The blood samples were placed into 100 ml glass bottles containing 1.2 mg/ml of anhydrous salt of ethylene diamine tetra acetic acid.

2.3. *Flow cytometry experiments*

The whole blood analysis was carried out with a MAXM hematology flow cytometry system (Beckman Coulter, USA). The system is calibrated with the reference blood on a daily basis. The

cell number and cell volume analyses were carried out according to the Coulter principle. The error bars in Figures 1 and 2 are incorporated in terms of ± standard deviations of RBC and MCV counts at each point measurement. Each point designates at least four replicates of each HHP treatment.

2.4. *Light microscopy*

After the HHP treatment, the samples were stained with the Wright Solution. A Zeiss KS 400 Image Analysis System was used to observe the stained cells.

2.5. *Atomic force microscopy*

The AFM experiments were carried out using an MMAFM-2/1700EXL model instrument within the contact mode. The whole blood samples were fixed on the glass slide surfaces and allowed to dry. Then, the glass slides were cut into appropriate sizes to fit the device holder and the samples were analyzed.

2.6. *Pretreatment of blood cells prior to the FTIR study*

The whole blood was spun at 2000 rpm for 10 min at room temperature. The plasma part was discarded without disturbing the "buffy coat" layer and the rest of the mixture was then mixed to obtain a homogenous sample.

2.7. *FTIR spectrum accumulation and data processing*

Spectral acquisition was carried out with a Perkin-Elmer spectrometer equipped with a MIR TGS detector (Spectrum One Instrument, Perkin-Elmer). FTIR spectra of the samples were recorded between the 4000 and 450 cm^{-1} region. Blood cell samples of 4 μl were placed between water-insoluble ZnSe windows with 6 mm sample thickness. Interferograms were averaged for 50 scans at 4 cm^{-1} resolution. The background spectrum was subtracted from the spectra of

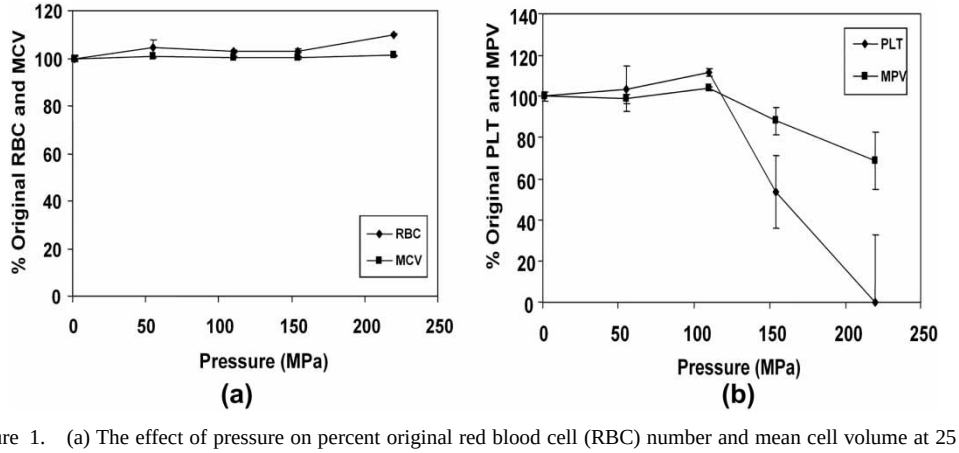

Figure 1. (a) The effect of pressure on percent original red blood cell (RBC) number and mean cell volume at 25 °C for 5 min of HHP treatment, RBC: red blood cell number, MCV: mean cell volume for RBCs. (b) The effect of pressure on percent original platelet number and mean platelet volume at 25 °C for 5 min of HHP treatment, PLT: platelet number, MPV: mean platelet volume.

the samples automatically. Spectrum One (Perkin-Elmer) software was used for all of the data manipulations.

From each sample, at least three different scans were obtained and these spectra, scanned under the same conditions, were identical. These replicates were averaged and the averaged spectra for each sample were then used for further data manipulation and statistical analysis. The spectrum of each pressure-treated sample was resolved by the subtraction of the spectrum of water, which gives strong absorption bands overlapping with the bands of interest in this study. The spectra were first interactively baseline corrected with respect to two arbitrarily selected points. Then, the spectra were normalized in specific regions for visual comparison of the HHP-treated and control samples.

2.8. *Artificial neural network analysis of amide-I band*

The amide-I band of the control and pressure-treated samples were analyzed and protein secondary structure was predicted through the software developed by Severcan et al. [18]. Neural networks were first trained using FTIR spectra of 18 water soluble proteins recorded in water [19] whose secondary structures were known from X-ray crystallography. Amide-I band, namely absorption values from 1600–1700 cm^{-1}, was preprocessed before applying to the neural networks. Preprocessing involves normalization and discrete cosine transformation (DCT) of the amide-I band of the FTIR spectra. To improve the training of the neural networks, the size of the training data set was increased by interpolating the available FTIR spectra. The NNs were trained using Bayesian regularization. For each structure parameter, a separate NN was trained whose number of inputs, i.e. the number of DCT coefficients, and number of hidden neurons were optimized. The trained NNs have standard error of prediction values of 4.19% for α-helix, 3.49% for β-sheet and 3.15% for turns. The secondary structure parameters of the new proteins were predicted by applying to the inputs of the trained NNs the preprocessed FTIR data. The details of the training and testing algorithm can be found in Severcan et al. [18].

2.9. *Statistical analysis*

The differences between the control and pressure-treated groups were compared using Mann–Whitney U Test with the Minitab Statistical Software Release 13.0 program. The statistical results are expressed as means $\pm$ standard deviation and P values of less than 0.05 were considered statistically significant.

3. Results

The blood cells were treated with 55, 110, 154 and 220 MPa pressure. Flow cytometry, light microscopy, AFM and FTIR spectroscopy experiments were carried out to see any detrimental effects of HHP treatment on the RBCs and platelets.

3.1. *Flow cytometry studies*

Figure 1(a) shows the results of the flow cytometry studies indicating that RBCs are very stable even at 154 MPa pressure in terms of the RBC number and volume measurements. The effect of high pressure on the mean RBC volume was also tested for the mentioned pressure levels (Figure 1(a)). The results showed that there is no effect of HHP on RBC volume over the pressure

range studied, suggesting that the RBCs retain their structure and shape under this range of pressure.

The effect of HHP on the platelet number was also measured in the experiments with the whole blood samples (Figure 1(b)). In terms of platelet number and volume, the results revealed that platelets are stable up to 110 MPa pressure, but they lose their structure above that pressure. The platelet number decreased about 50% at 154 MPa and the destruction was apparent at 220 MPa. When compared with the structure of RBCs, they turned out to be quite unstable to pressures of 154 MPa and above. As seen from the same figure, a similar trend was also observed for mean platelet volume for control and HHP-treated samples. In either case, both the platelet number and the mean platelet volume decreased at HHP treatments greater than 110 MPa. This experiment showed the fragility of the platelet structure above 110 MPa.

3.2. *Light microscopy studies*

Light microscopy experiments were carried out to see pressure-induced variations on the red cells of the blood. Figure 2 shows the effect of high pressure on RBC morphology using light microscopy. As seen from the figure, the overall shapes of RBCs remain stable up until the 220 MPa pressure treatments for the designated time intervals. Small protrusions were observed at 220 MPa.

3.3. *AFM studies*

AFM experiments, results of which can be seen in Figure 3, were carried out to see morphological changes on the RBCs in detail. No change in the appearances of the RBCs after a 5-min pressure application of 132 MPa (data not shown) was observed. However, when the pressure level was raised to 220 MPa the change on the surface morphology was apparent.

3.4. *FTIR spectroscopy studies*

The FTIR spectroscopy technique provides useful information about the structure and function of the macromolecular constituents of biological systems at molecular level [15,16,20,21]. The FTIR spectrum of blood cells is quite complex and consists of several bands originating from the contribution of different functional groups belonging to biomolecules, such as lipids and proteins. Therefore, the spectra were analyzed for the following spectral regions: 2830–3015 and 1141–1361 cm^{-1} for the analysis of lipids and 1600–1700 cm^{-1} for the analysis of proteins. It should be emphasized that all the spectra presented in the figures were normalized with respect to

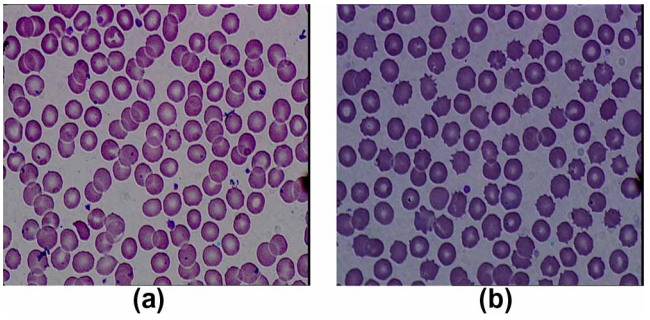

Figure 2. The effect of HHP treatment on RBC morphology studied with light microscopy; (a) Control, (b) 220 MPa, ×1000.

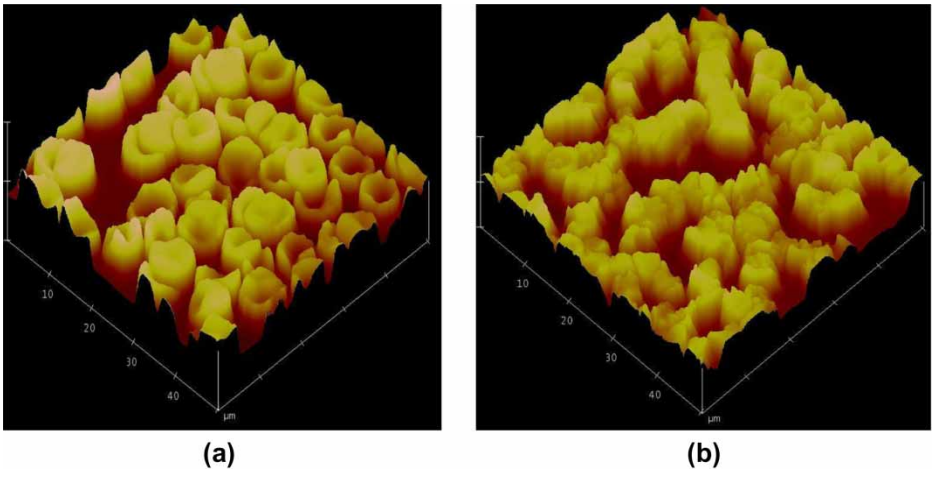

Figure 3. The effect of HHP treatment on RBC surface morphology studied with AFM; (a) Control, (b) 220 MPa scales are in μm.

specific selected bands, but these spectra were used only for illustrative purposes. However, each original baseline-corrected spectrum belonging to the corresponding control and treated groups was considered separately during the accurate measurement of the spectral parameters.

3.4.1. *2830–3015 cm^{-1} region*

Figure 4(a) shows the average FTIR spectra of control and HHP-treated blood cells in the 2830–3015 cm^{-1} spectral region. The FTIR spectrum in this region consists of four bands: the CH_3 asymmetric stretching band located at 2959 cm^{-1}, which has contributions from both lipids and proteins [16], the CH_2 asymmetric stretching band located at 2936 cm^{-1} and CH_2 symmetric stretching band located at 2852 cm^{-1}, which are mainly due to lipids [22] and the CH_3 symmetric stretching band located at 2872 cm^{-1}, which mainly monitors proteins [22]. All the control and treated spectra have almost the same overlapping absorption bands. No change was observed in the wavenumber, intensity and bandwidth values of the bands as seen from the figure.

3.4.2. *1141–1361 cm^{-1} region*

Figure 4(b) shows the average FTIR spectra of control and HHP-treated blood cells in the 1141–1361 cm^{-1} spectral region. The band of interest in this region is the one located around 1170 cm^{-1}, which is due to CO–O–C asymmetric stretching vibration of ester bonds in cholesterol esters [23]. The area of this band decreased slightly for the 132 MPa treatments, but significantly ($P < 0.05$) for the 220 MPa treatments as seen in Figure 4(c).

3.4.3. *1600–1700 cm^{-1} (Amide-I) region*

Figure 4(d) shows the second derivative of the baseline-corrected normalized average FTIR spectra of control and HHP-treated blood cells in the 1600–1715 cm^{-1} region. Unresolved secondary structure elements are clearly seen in the second derivative spectra. Every minimum point in the second derivative spectrum corresponds to a maximum point in the absorbance spectrum. The gradual loss in the intensity of the peak located at 1681 cm^{-1} with the corresponding increase in pressure level is noticeable in the spectra as seen from Figure 4(e).

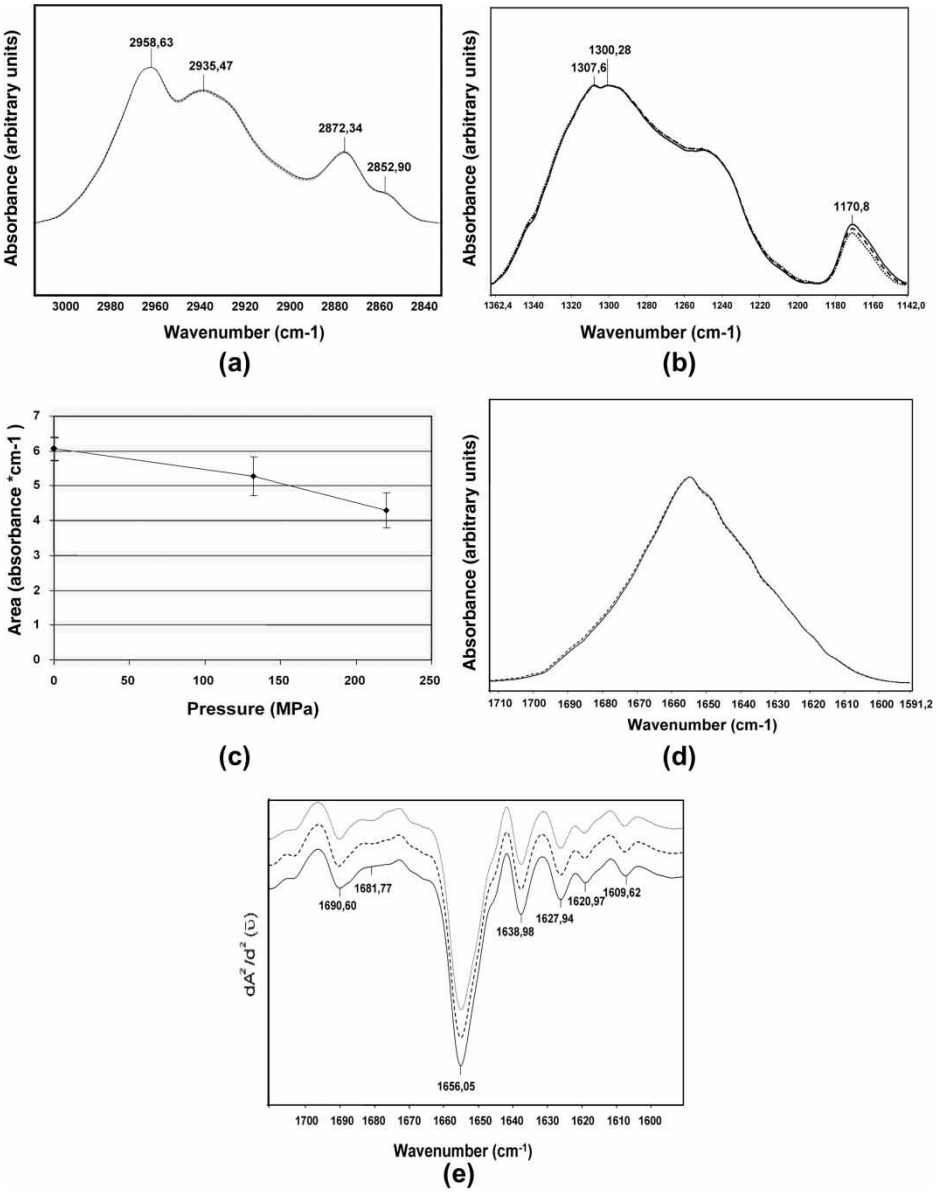

Figure 4. (a) The average FTIR spectra of control (solid line), 132 MPa (dashed line) and 220 MPa (dotted line) HHP-treated blood cells in the 3010–2830 cm^{-1} region (spectra were normalized with respect to the 2958 cm^{-1} band). (b) The average FTIR spectra of control, 132 MPa and 220 MPa HHP-treated blood cells in the 1361–1141 cm^{-1} region (spectra were normalized with respect to the 1307 cm^{-1} band). (c) The average area under the 1170 band for the control, 132 and 220 MPa HHP treatments. (d) The average FTIR spectra of control, 132 MPa and 220 MPa HHP-treated blood cells in the amide-I region (spectra were normalized with respect to the 1656 cm^{-1} band). (e) The second derivatives of the average FTIR spectra of control, 132 MPa and 220 MPa HHP-treated blood cells in the amide-I region (the spectra were normalized with respect to the 1656 cm^{-1} band).

3.5. *Analysis of protein secondary structure elements with an artificial neural network algorithm based on FTIR data*

An artificial neural network algorithm was used to predict the relative amounts of several secondary structural elements of blood cells for different pressure levels, whose results are shown in Figure 5.

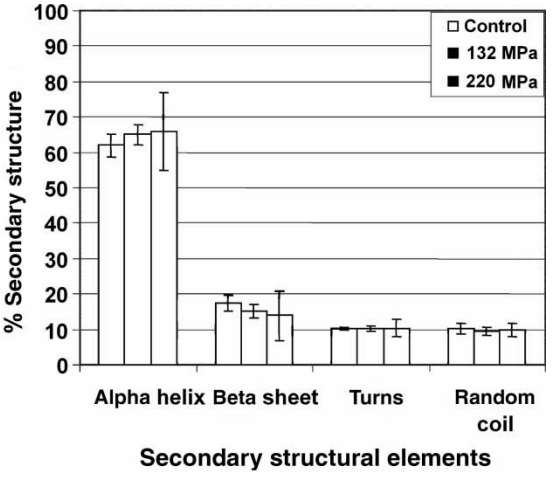

Figure 5. The effect of HHP on the secondary structural elements of blood cells studied by the artificial neural network algorithm method.

As seen from the figure, high-pressure treatment slightly increased α-Helix content and slightly decreased β-Sheet structure. However, these changes were found to be statistically insignificant.

4. Discussion

In this work, we studied the effect of HHP on the stability behavior of blood cells by flow cytometry, light microscopy, AFM and FTIR spectroscopy. These techniques were used to understand whether high pressure induced any effects on the structure of RBCs and platelets, or not.

The results of the flow cytometry study indicated the stability of RBCs against HHP up until a pressure of 220 MPa. They showed only subtle changes in their morphology at 220 MPa (Figure 2). The AFM study of the RBCs in the 220 MPa treatments showed small perturbations on their surfaces (Figure 3) that were not clearly detectable under the light microscope.

The flow cytometry study indicated that platelets are not stable above 154 MPa. Their number rapidly decreased at these pressure levels. The results indicated that their cell membranes were more fragile against pressure effects. This instability indicated that the maximum pressure level that can be applied to the whole blood should be considered to be around 110 MPa. The platelet cell volumes also showed a similar decrease after an identical pressure application (Figure 1(b)). The differences in the stability behavior of the RBC and platelet membranes should be due to their structural differences.

The effect of HHP treatment on the RBC shape was investigated by light microscopy and AFM, both of which revealed similar results. HHP treatment at 220 MPa created bulges on the surface of the RBCs. Similarly, AFM results also supported this observation and indicated that the pressure-treated RBCs were merged. The microscopic studies used in the present study proposed a kind of "softening" in the structure of the RBCs, which are the most abundant cell type in the blood. It is not possible to understand the nature of such a morphological change without using molecular biochemical/biophysical techniques, such as FTIR spectroscopy.

FTIR spectroscopy enabled us to rapidly and sensitively monitor pressure-induced structural alterations in lipids and proteins in untreated, unstained and unfixed whole-tissue samples without destroying the native structure of the proteins. In FTIR studies, the signal intensity and area under the bands give information about the concentration of the related functional groups [24].

The frequency (wavenumber) of the CH_2 stretching bands gives information about acyl chain flexibility, which is a structural parameter monitoring lipid order/disorder [16]. The bandwidth of the lipid bands in the same region monitors lipid dynamics [25,26].

The FTIR spectroscopic study of the control and HHP-treated blood cells revealed that no change in the lipid order and dynamics was observed due to HHP treatment. The results also showed that the HHP application does not change the lipid and total protein concentrations, with the exception of the area under the 1170 cm^{-1} band. This band is due to CO–O–C asymmetric stretching vibrations of ester bonds in cholesterol esters [23]. The decrease in the area of the 1170 cm^{-1} band at all pressure treatments, with greater significance at 220 MPa, indicates a gradual loss in cholesterol esters in the system due to HHP treatment. Rigas et al. [27] studied this band for human colorectal cancer tissues at different pressures in an anvil cell. They observed a shift towards lower frequencies and a differentiation in shape upon HHP treatment. The decrease observed in the cholesterol concentration for HHP-treated samples is important because cholesterol is also proposed to facilitate a fluid–fluid lateral phase separation of glycerophospholipid- and sphingolipid-enriched phases into separate domains in the liquid crystalline phase [28]. The presence of similar domains after or during HHP treatment is well known. Kusube et al. [29] indicated that HHP treatment can impose phase transitions in model membrane structures, using differential scanning calorimetry and high-pressure optical tools. Similarly, Tauc et al. [30] presented that small changes in temperature/pressure and/or cholesterol concentration perturb the local fraction and composition of cholesterol domains, using dynamic fluorescence spectroscopy.

We obtained information about the protein secondary structural changes monitoring the variations in the intensity of the sub-bands in the amide-I region. Signal intensity of the second derivative infrared bands has previously been used to obtain information about the relative concentration changes of macromolecules [31,32]. We have observed a gradual loss in the intensity of the 1681 cm^{-1} band, which mainly monitors anti-parallel β-sheet structure [33]. However, its precise assignment is often difficult because of the overlapping absorption of β-turn and unordered structures [34–36]. For the homopolypeptide poly-L-lysine, a weaker band associated with high-frequency vibration of anti-parallel β-sheet structure is seen at 1680 cm^{-1} [34]. The gradual loss in this 1681 cm^{-1} band is consistent with NN studies, which revealed a loss in β-sheet structure with increasing pressure. No pressure-induced change was observed in the turn structure, as can be seen from Figure 5. In recent years, neural networks have proven to be a reliable method used for the prediction of protein secondary structure content [37–39]. The results of the neural network analysis in this study suggest that high pressure causes slight alterations in the protein secondary structure by increasing the α-helix and decreasing the β-sheet contents. However these changes were found to be insignificant.

Since, in our experiments, erythrocytes were observed to be sensitive to elevated HHP treatments as high as 220 MPa with AFM, we suspected that HHP treatment may have adverse effects on the elements of the cytoskeleton. Similarly, Ishii et al. [40] found that HHP directly affects cell survival and morphology through the dissociation of the cytoskeletal frameworks, using indirect immunofluorescence microscopy. It was also previously reported that elevated pressure alters the distinctive cell shapes of eukaryotic cells into simple round ones, and the structures of cytoskeletal proteins, such as microtubules, are depolymerized *in vivo* and *in vitro* [41]. In addition, the light microscopy results of the referred study revealed that HHP treatment in *Escherichia coli* leads to the formation of irregular elongated structures other than their normal phenotype.

In this study, the light microscopy and AFM studies revealed morphological alterations upon exposure to HHP treatments. The changes in the shapes of RBCs and platelets and the changes in the cholesterol band areas indicate two possible kinetic pathways of HHP-induced structural alterations as sketched in the following figure.

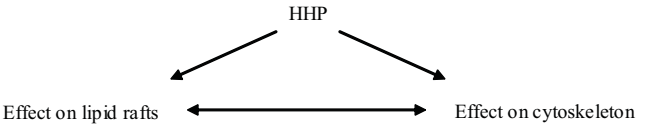

According to the figure above, after the HHP treatment, the changes in the cytoskeleton might be triggering the changes in the erythrocyte membrane topology through lipid rafts or both changes occurring simultaneously.

In conclusion, the results of this study indicate that HHP treatment does not cause significant changes in protein and lipid structure, composition and concentration of the blood-cell constituents except cholesterol in the investigated pressure area. However, the results revealed the evidence of morphological alterations due to HHP treatment.

Acknowledgements

This study was financially supported by Middle East Technical University, Turkey, Grant No: BAP-2004-07-02-00-48. We would like to thank Nusret Taheri for allowing us to use the flow cytometer in the Medical Center of METU and Prof. Dr Aykut Özkul for his helpful discussions.

References

[1] D. Knorr, *Effects of high-hydrostatic-pressure processes on food safety and quality*, Food Technol. Chic. 47 (1993), pp. 156–161.
[2] L.A. Tedford, D. Smith, and C.J. Schaschke, *High pressure processing effects on the molecular structure of ovalbumin, lysozyme and β-lactoglobulin*, Food Res. Int. 32 (1999), pp. 101–106.
[3] D.G. Hoover, C. Metrick, A.M. Papineau, D.F. Farkas, and D. Knorr, *Biological effects of high hydrostatic pressure on food microorganisms*, Food Technol. Chic. 43 (1989), pp. 99–107.
[4] Y. Goldman and M. Shinitzky, *Immunotheraphy of cancer with a pressurized, surface reduced tumor-cell vaccine*, Drug Develop. Res. 50 (2000), pp. 272–284.
[5] J.A. Kornblatt and M.J. Kornblatt, *The effects of osmotic and hydrostatic pressures on macromolecular systems*, Biochim. Biophys. Acta 1595 (2002), pp. 30–47.
[6] K. Heremans and L. Smeller, *Protein structure and dynamics at high pressure*, Biochim. Biophys. Acta 1386 (1998), pp. 353–370.
[7] J.L. Silva, *High Pressure Chemistry, Biochemistry and Material Sciences, NATO ASI Series*, Vol. 401, R. Winter and J. Jonas, eds., Kluwer Academic Publishers, Dordrecht, The Netherlands, 1993, pp. 561–578.
[8] A.T. Da Poian, J.E. Johnson, and J.L. Silva, *Differences in pressure stability of the three components of cowpea mosaic virus: implications for virus assembly and disassembly*, Biochem. US 33 (1994), pp. 8339–8346.
[9] E. Jurkiewicz, M. Villas-Boas, J.L. Silva, G. Weber, G. Hunsmann, and R.M. Clegg, *Inactivation of simian immunodeficiency virus by hydrostatic pressure*, Proc. Natl. Acad. Sci. USA 92 (1995), pp. 6935–6937.
[10] D.W. Bradley, R.A. Hess, F. Tao, L.Sciaba-Lentz, A.T. Remaley, J.A. Laugharn, and M. Manak, *Pressure cycling technology: a novel approach to virus inactivation in plasma*, Transfusion 40 (2000), pp. 193–200.
[11] E. Saguer, E. Davila, M. Toldra, N. Fort, S. Baixas, C. Carratero, and D. Pares, *Effectiveness of high pressure processing on the hygienic and technological quality of porcine plasma from biopreserved blood*, Meat. Sci. 76 (2007), pp. 189–193.
[12] M. Toldra, A. Elias, D. Pares, E. Saguer, and C. Carretero, *Functional properties of a spray-dried porcine red blood cell fraction treated by high hydrostatic pressure*, Food Chem. 88 (2004), pp. 461–468.
[13] M. Toldra, E. Davila, E. Saguer, N. Fort, P. Salvador, D. Pares, and C. Carretero, *Functional and quality characteristics of the red blood cell fraction from biopreserved porcine blood as influenced by high pressure processing*, Meat Sci. 80 (2008), pp. 380–388.
[14] A.M. Matser, C. Van Der Ven, C.W.N. Gouwerok, and D. De Korte, *High-pressure processing for preservation of blood products*, High Press. Res. 25 (2005), pp. 37–41.
[15] A. Dogan, K. Ergen, F. Budak, and F. Severcan, *Evaluation of disseminated candidiasis on an experimental animal model: a Fourier transform infrared study*, Appl. Spectrosc. 61 (2007), pp. 199–203.
[16] G. Cakmak, I. Togan, and F. Severcan, *17β-Estradiol induced compositional, structural and functional changes in rainbow trout liver, revealed by FT-IR spectroscopy: a comparative study with nonylphenol*, Aquat. Toxicol. 77 (2006), pp. 53–63.
[17] V.M. Balasubramaniam, E.Y. Ting, C.M. Stewart, and J.A. Robbins, *Recommended laboratory practices for conducting high-pressure microbial inactivation experiments*, Innovat. Food Sci. Emerg. Tech. 5 (2004), pp. 299–306.

[18] M. Severcan, P.I. Haris, and F. Severcan, *Using artificially generated spectral data to improve protein secondary structure prediction from Fourier transform infrared spectra of proteins*, Anal. Biochem. 332 (2004), pp. 238–244.
[19] M. Severcan, F. Severcan, and P.I. Haris, *Estimation of protein secondary structure from FTIR spectra using neural networks*, J. Mol. Struct. 565–566 (2001), pp. 383-387.
[20] F. Severcan and P.I. Haris, *Fourier transform infrared spectroscopy suggests unfolding of loop structures precedes complete unfolding of pig citrate*, Biopolymers 69 (2003), pp. 440–447.
[21] N. Toyran, F. Zorlu, and F. Severcan, *Effect of stereotactic radiosurgery on lipids and proteins of normal and hypoperfused rat brain homogenates: a Fourier transform infrared spectroscopy study*, Int. J. Radiat. Biol. 81 (2005), pp. 911–918.
[22] F. Severcan, N. Toyran, N. Kaptan, and B. Turan, *Fourier transform infrared study of the effect of diabetes on rat liver and heart tissues in the C-H region*, Talanta 53 (2000), pp. 55–59.
[23] M. Jackson, B. Ramjiawan, M. Hewko, and H.H. Mantsch, *Infrared microscopic functional group mapping and spectral clustering analysis of hypercholesterolemic rabbit liver*, Cell. Mol. Biol. 44 (1998), pp. 89–98.
[24] D. Freifelder, *Physical Chemistry*, Chapter 14, W. H. Freeman and Company, New York, 1982.
[25] H. Boyar and F. Severcan, *Oestrogen-phospholipid membrane interactions: an FTIR study*, J. Mol. Struct. 408–409 (1997), pp. 269–272.
[26] C. Schultz and D. Naumann, *In vivo study of the state of order of the membranes of gram-negative bacteria by fourier-transform infrared spectroscopy (FT-IR)*, FEBS Lett. 294 (1991), pp. 43–46.
[27] B. Rigas, S. Morgello, I.S. Goldman, and P.T.T. Wong, *Human colorectal cancers display abnormal fourier-transform infrared spectra*, Proc. Natl. Acad. Sci. USA 87 (1990), pp. 8140–8144.
[28] B. Ramstedt and J.P. Slotte, *Sphingolipids and the formation of sterol-enriched ordered membrane domains*, Biochim. Biophys. Acta 1758 (2006), pp. 1945–1956.
[29] M. Kusube, H. Matsuki, and S. Kaneshina, *Thermotropic and barotropic phase transitions of N-methylated dipalmitoylphosphatidylethanolamine bilayers*, Biochim. Biophys. Acta 1668 (2005), pp. 25–32.
[30] P. Tauc, C.R. Mateo, and J. Brochon, *Investigation of the effect of high hydrostatic pressure on proteins and lipidic membranes by dynamic flourescence spectroscopy*, Biochim. Biophys. Acta 1595 (2002), pp. 103–115.
[31] N. Toyran, P. Lasch, D. Naumann, B. Turan, and F. Severcan, *Early alterations in myocardia and vessels of the diabetic rat heart: an FTIR microspectroscopic study*, Biochem. J. 397 (2006), pp. 1–10.
[32] N. Toyran, B. Turan, and F. Severcan, *Selenium alters the lipid content and protein profile of rat heart: An FTIR microspectroscopic study*, Arch. Biochem. Biophys. 458 (2007), pp. 184–193.
[33] S. Choi and C. Ma, *Conformational study of globulin from common buckwheat (*Fagophyrum esculentum *Moench) by Fourier transform infrared spectroscopy and differential scanning calorimetry*, J. Agr. Food Chem. 53 (2005), pp. 8046–8053.
[34] P.I. Haris and F. Severcan, *FTIR spectroscopic characterization of protein structure in aqueous and nonaqueous media*, J. Mol. Catal. B Enzymatic 7 (1999), pp. 207–221.
[35] A. Troullier, D. Reinstadler, Y. Dupont, D. Neymann, and V. Forge, *Transient non-native secondary structures during the refolding of α-lactalbumin detected by infrared spectroscopy*, Nat. Struct. Biol. 7 (2000), pp. 78–86.
[36] N. Wellner, P.S. Belton, and S. Tathami, *Fourier transform IR spectroscopy of hydration induced structure changes in the solid state of w-gliadins*, Biochem. J. 319 (1996), pp. 741–747.
[37] G.J. Barton, *Protein secondary structure prediction*, Curr. Opin. Struc. Biol. 5 (1995), pp. 372–376.
[38] G. Bohm, *New approaches in molecular structure prediction*, Biophys. Chem. 59 (1996), pp. 1–32.
[39] J.A. Hering, P.R. Innocent, and P.I. Haris, *Neuro-fuzzy structural classification of proteins for improved secondary structural classification of proteins*, Proteomics 3 (2003), pp. 1464–1475.
[40] A. Ishii, T. Sato, M. Wachi, K. Nagai and C. Kato, *Effects of high hydrostatic pressure on bacterial cytoskeleton FtsZ polymers* in vivo *and* in vitro, Microbiology+ 150 (2004), pp. 1965–1972.
[41] E.D. Salmon, D. Goode, T.K. Maugel, and D.B. Bonar, *Pressure-induced depolymerization of spindle microtubules III differential stability in HeLa cells*, J. Cell. Biol. 69 (1976), pp. 443–454.